Catalysis Today 196 (2012) 3–10

Contents lists available at SciVerse ScienceDirect

Catalysis Today

journal homepage: www.elsevier.com/locate/cattod

Catalytic hydroprocessing of lignin under thermal and ultrasound conditions

Kenneth B.H. Finch[a], Ryan M. Richards[a], Aurore Richel[b], Andrei V. Medvedovici[c], Nicoleta G. Gheorghe[d], Marian Verziu[e], Simona M. Coman[e], Vasile I. Parvulescu[e,*]

[a] Department of Chemistry and Geochemistry, Colorado School of Mines, 304 Coolbaugh Hall, 1012 14th St, Golden, CO 80401, USA
[b] Unit of Biological and Industrial Chemistry, University of Liege – Gembloux Agro-Bio Tech, Passage des Déportés, 2 – B-5030 Gembloux, Belgium
[c] Department of Analytical Chemistry, Faculty of Chemistry, University of Bucharest, Bdul Regina Elisabeta, 4-12, Bucharest 030016, Romania
[d] National Institute of Materials Physics, Atomistilor 105b, 077125 Magurele-Ilfov, Romania
[e] Department of Organic Chemistry, Biochemistry and Catalysis, Faculty of Chemistry, University of Bucharest, Bdul Regina Elisabeta, 4-12, Bucharest 030016, Romania

ARTICLE INFO

Article history:
Received 31 October 2011
Received in revised form 6 January 2012
Accepted 12 February 2012
Available online 21 March 2012

Keywords:
Lignin
Alkaline treatment
Acidic treatment
Depolymerization
Nano-catalysts
Low-molecular compounds

ABSTRACT

Lignin isolated from *Miscanthus* × *giganteus* using acidic (FAL) and basic (AL) conditions was thereafter subjected to catalytic depolymerization under thermal or ultrasonic activation. The characterization of lignin samples was achieved by thermogravimetric analysis and FTIR. Three different classes of catalysts containing nickel as the active species have been prepared in this respect: (i) nano-Ni(0) by reduction of $NiCl_2$ with $NaBH_4$ under ultrasonication, (ii) Fe_3O_4–$(NiMgAlO)_x$ and $(NiAlO)_x$ by calcination of Mg(Ni)–Al hydrotalcite incorporating Fe_3O_4, followed by reduction with hydrogen, and (iii) NiO(1 1 1) nanosheets by reduction of $Ni(NO_3)_2$ with urea using benzyl alcohol as a structure directing agent. The catalysts were characterized by XRD and XPS techniques. Reduced mixed oxides displayed a moderate activity while a significant increase in conversion (up to 90%) was observed with nano-Ni(0) and NiO(1 1 1) nanosheets catalysts. The conversion and the mass distribution of the reaction products were strongly related to the procedure used for the extraction of lignin. In all the reactions AL samples had a greater extent of depolymerization. The performance from the tested catalysts under ultrasonic conditions was inferior to those tested under conventional heating conditions. The nature of the solvent was also found to be very important to this process, with the ionic liquid, 1-butyl-3-methylimidazolium acetate ([BMIM]OAc) demonstrating the best results in autoclave conditions and methanol under ultrasonic conditions.

1. Introduction

The continual consumption of petroleum reserves and the growing concerns over the emission of greenhouse gases have stimulated intense research to investigate the potential of biomass as a renewable alternative for fuel and/or chemical production.

Currently, lignocellulose is the most abundant component of biomass (20–28% tree composition) and is composed of three types of polymers: cellulose, hemicelluloses and lignin. Lignin is potentially an important renewable raw material for the production of multiple products including fuels and high-value chemicals. However, depolymerization of lignin (composed from different phenylpropene monomer units as coniferyl, sinapyl and *p*-coumaryl alcohol [1]) is not an easy task and many efforts are focused on this challenge. The reported methods to convert this natural aromatic polymer into smaller molecules utilize such thermochemical treatments as pyrolysis, hydrogenolysis, hydrolysis, gasification and oxidation [2–7]. Pyrolysis of lignin leads to oils, gases as well as solid char. The proportion of these products depends on several factors such as feedstock type [8], heating rate, reaction temperature [2] and the presence or absence of a catalyst [9]. Mullen and Boateng [9] showed that in the presence of the catalysts HZSM-5 or CoO/MoO_3 the aromatic fraction is increased at 650 °C. In supercritical water with Ni/MgO or Co/MgO the selectivity of the reaction changes in favor of the production of hydrogen and the performance depends on the catalyst calcination temperature [10]. Depolymerization of wheat stalk powder was also carried out in supercritical ethanol using CaO/Al_2O_3 and $CaO/Al_2O_3/Fe_3O_4$ catalysts [11]. The presence of these catalysts increased the conversion from 12.0% without a catalyst to 29.0% using CaO/Al_2O_3 and 42.4% using $CaO/Al_2O_3/Fe_3O_4$.

Oxidation of lignin may also offer a versatile route to aromatic aldehydes. A $LaFe_{1-x}Cu_xO_3$ catalyst was shown to enhance the selectivity and could be recycled for several runs without significant deactivation [12]. In the absence of a heterogeneous catalytic species, a pH close to 14 must be employed to obtain similar results [13]. However, such conditions are difficult from both an economic

* Corresponding author. Tel.: +40 21 4100241; fax: +40 21 4100241.
E-mail addresses: simona.coman@g.unibuc.ro (S.M. Coman), vasile.parvulescu@g.unibuc.ro (V.I. Parvulescu).

0920-5861/$ – see front matter © 2012 Elsevier B.V. All rights reserved.
doi:10.1016/j.cattod.2012.02.051

and an environmental point of view. Dissolving lignin in ionic liquids [14] followed by oxidation over transition metals [15] may present an alternative route to aromatic aldehydes.

Noble metals can also catalyze the conversion of lignin into alkanes and methanol in a two step process. First, the conversion of lignin to monomers and dimers was achieved by a catalytic cleavage of the C–O–C bonds (without disrupting the C–C linkages) using a series of catalysts carbon supported including Ru/C, Pd/C, Rh/C and Pt/C, under modest H_2 pressures. Subsequently, the obtained monomers and dimers were further hydrogenated over Pd/C with good yields of alkanes and methanol [16]. The main drawback of this process is the high price of the noble metals.

The solvation of lignin is important to achieve a high conversion rate. It has been demonstrated that certain ionic liquids can be used as "green" aprotic solvents for lignin. For the $[BMIM]^+$ – containing ionic liquids, Ragauskas et al. [14] have shown that the solvation of lignin varies with the anion in the order: $[MeOSO_3]^- > Cl^- > Br^- \ggg [PF_6]^-$ indicating that the solubility of lignin was principally influenced by the nature of the anions. Ionic liquids containing large, non-coordinating anions $[PF_4]^-$ and $[PF_6]^-$ were unsuitable as a solvent for lignin.

The aim of the present study was to depolymerize lignin under mild conditions (thermal (e.g., autoclave) and ultrasound conditions), using nickel as the active species in both the reduced (Ni) and oxidized state ($(NiAlO)_x$ and $(NiMgAlO)_x$). For comparison, NiO(1 1 1) nanosheets with hexagonal holes [17] have been tested in the same reaction. The catalytic experiments were carried out in autoclave and ultrasounds activation conditions using as solvents water, organic solvents and ionic liquids. Another scope of this study was to optimize the analytical conditions for an accurate characterization of the process.

2. Experimental

2.1. Lignin preparation

Miscanthus × *giganteus* from a crop cultivated in spring 2007, and harvested after two years (Tournai, Belgium) was used as the raw material after the stems were stripped of leaves, air-dried and ensiled. The material was ground into 1–2 mm particles. The untreated *Miscanthus* was mainly composed of 24.5% lignin, 48.4% glucose, 15.7% xylose, 1.9% arabinose, 1.2% galactose, 0.2% mannose, 6.4% extractives and 2.4% ash [18].

The extraction of lignin from *Miscanthus* × *giganteus* was carried out using either a formic acid/acetic acid/water mixture (acidic medium) or an aqueous ammonia solution (25 wt%) (basic medium). The protocol used for the extraction of lignin in acidic medium was based on a methodology described by Lam et al. [19] with some modifications: the dry lignin was soaked at 50 °C for 30 min in a formic acid/acetic acid/water mixture (30/50/20, vol/vol/vol ratio) and then the temperature was increased to 107 °C for 3 h with continuous agitation. The ratio of dry matter to soaking liquid was 1/25. After cooling, the pulp was filtered out with the aid of a vacuum filter funnel (500 mL, 95 mm diameter) assembled with a fritted disk (40–100 μm pore size Robu Glasfilter-Geräte GmbH) to black liquor. Recovery of lignin was done by precipitation from black liquor by adding H_2SO_4 (72%, w/w) until a pH of 1.5 was reached. The precipitated lignin was then isolated by centrifugation and dried using a lyophilization technique. The obtained sample is named FAL (Formic Acid Lignin).

The extraction of lignin in basic medium occurred by soaking raw material with an ammonia aqueous solution (25 wt.%) at 60 °C for 6 h in a water bath [18]. The ammonia from black liquor obtained after pulp filtration was vacuum-evaporated at 40 °C. The recovery of lignin was accomplished by using a method similar to the FAL sample, centrifugation followed by lyophilisation. The obtained sample is named AL (Ammonia Lignin).

2.2. Catalyst preparation

The nano-Ni catalyst was prepared by adding 21.5 g $NiCl_2{\cdot}6H_2O$ dissolved in 300 mL methanol to a mixture of 27.5 mL $N_2H_4{\cdot}H_2O$, 26 mL distilled water and 2.5 g NaOH. The obtained mixture was ultrasonicated for 1.5 h in the presence of 0.8 g of $NaBH_4$. The formed black precipitate was thereafter washed with distilled water and dried at room temperature.

Fe_3O_4–$(NiMgAlO)_x$ and $(NiAlO)_x$ particles containing 30 wt%. Ni were prepared by calcination of Mg(Ni)–Al hydrotalcite precursors. An aqueous solution containing 1.92 g of $Ni(NO_3)_2{\cdot}6H_2O$, 2.56 g $Mg(NO_3)_2{\cdot}6H_2O$ and 2.06 g of $Al(NO_3)_3{\cdot}9H_2O$ or 5.82 g of $Ni(NO_3)_2{\cdot}6H_2O$ and 2.47 g of $Al(NO_3)_3{\cdot}9H_2O$ was added to a Fe_3O_4 suspension with a Ni/Fe molar ratio of 50. The obtained slurry was stirred at 60 °C and a 1 M solution of $NaOH/Na_2CO_3$ was added dropwise until a pH of 10 was reached. The resultant mixture was transferred into an autoclave and hydrothermally treated at 200 °C for 10 h. After cooling to room temperature, the obtained hydrotalcite was washed with distilled water to neutral pH, dried at 80 °C for 24 h, at 130 °C for 4 h and then calcined at 500 °C for 4 h in air [20]. Finally, the resulted mixed oxides were treated in a hydrogen flow (30 mL min^{-1}) at 180 °C for 3 h.

The NiO(1 1 1) nanosheets were prepared accordingly to a methodology described by Hu et al. [17]. 9 g of $Ni(NO_3)_2{\cdot}6H_2O$ was dissolved in 100 mL absolute methanol, then 1 g urea and 6.7 g benzyl alcohol were added, in the ratio Ni:urea:benzyl alcohol = 1:0.5:2 (molar ratio). After stirring for 1 h, the solution was transferred to an autoclave, purged with 7500 Torr Argon 5 times, before a pressure of 7500 Torr Argon was imposed prior to heating. The mixture was heated to 200 °C for 5 h, and then increased to 265 °C for 1.5 h. Finally, the reaction mixture was supercritically dried by allowing the solvent to vent at 265 °C. A green powder was collected and subsequently calcined in air at 500 °C for 6 h.

2.3. Catalyst and lignin characterization

The prepared catalysts were characterized using several techniques. XPS spectra were obtained at room temperature using a PHI 5600ci Multi Technique Instrument. The pressure in the analysis chamber was 1.33 mPa. Monochromatic AlKα radiation ($h\nu$ = 1486.6 eV) was generated by a beam current of 12 mA with an acceleration voltage of 10 kV. X-ray diffraction (XRD) patterns were obtained with a Shimadzu XRD 7000 diffractometer using CuKα radiation, from 5° to 90°. The crystallite size was determined from the X-ray line broadening using the Scherrer formula given by $D = 0.9\lambda/\beta\cos\theta$, where D is the average crystallite size, λ is the X-ray wavelength used (1.5406 Å), β is the angular line width of half maximum intensity and θ is the Bragg's angle in degree.

The extracted lignin samples (FAL and AL) were characterized by TG/TDA and FTIR techniques in order to investigate the effect of the pretreatments on the chemical structure and physico-chemical characteristics. Thermogravimetric analysis of the lignin samples was performed using a SDT Q600 instrument supplied by TA Instruments. The samples were placed in an alumina sample holder and heated at a rate of 5 °C min^{-1} from room temperature to 600 °C under N_2 atmosphere with a rate flow of 20 mL min^{-1}.

About 5 mg of dried lignin was mixed and ground with potassium bromide and then mechanically pressed into pellet form. FTIR spectra were obtained using a Bruker IFS 48 spectrometer from 2000 to 400 cm^{-1} with 16 scans at a resolution of 4 cm^{-1}.

2.4. Catalytic tests

Typical depolymerization experiments were carried out using 0.25 g lignin in 30 mL water or organic solvent (methanol, ethyl acetate) and 0.03 g catalyst while bubbling hydrogen under ultrasonic conditions for 6 h, at room temperature, using an Elma Transsonic 460/H bath at a frequency of 35 kHz. Alternatively, 0.16 g of lignin dissolved into 2 g [BMIM]OAc ionic liquid was heated to 180 °C under 1–10 atm of H_2 for 24 h with 0.02 g catalyst in an autoclave. [BMIM][OAc] was selected from a preliminary lignin solubility screening using the following IL's: 1-hexyl-3-methylimidazolium trifluoromethanesulfonate ([HMIM][CF3SO3]), 1-butyl-2,3-dimethylimidazolium tetrafluoroborate ([BM2IM][BF4]), 1-butyl-4-methylpyridinium hexafluorophosphate ([BMPY][PF6]), 1-butyl-3-methylimidazolium hexafluorophosphate ([BMIM][PF6]), 1-butyl-3-methylimidazolium chloride ([BMIM][Cl], 1-butyl-3-methylimidazolium bromide ([BMIM][Br], and 1-butyl-3-methylimidazolium acetate ([BMIM][OAc]).

After the ultrasonic experiments in water, the unreacted lignin was recovered by centrifugation of the mixture at 6000 rpm for 10 min. In the case of ionic liquid and organic solvents, after reaction the non-transformed lignin was precipitated by adding distilled water and separated by centrifugation.

The conversion of lignin to low molecular weight compounds was calculated using Eq. (1):

$$C\% = 100 - \left(\frac{m_i - m_f}{m_i} \times 100\right) \quad (1)$$

where m_i, mass of lignin introduced in reaction; m_f, mass of lignin recovered after reaction.

The analysis of the reaction products was made using LC–MS technique using an Agilent 1100 Series LC/MS equipped with a degasser (model G1379A), quaternary pump (model G1311A), automated injector (model G1329A), autosampler thermostat (model G1330BA), column thermostat (model G1316A), detector DAD (model G1315B), detector Triple Quad LC/MS (model G2445D), interface APCI (model G1947A), interface ESI (model G1948A), and column: Zorbax Eclipse XDB C18, lengh 50 mm, 4.6 mm i.d., 1.8 μm d.p. (sterically protected with di-isobutyl n-octadecylsilane). The operating conditions were temperature 25 °C, mobile phase: solvent A: aq. 0.1% formic acid and solvent B: 0.1% formic acid in acetonitrile, gradient profile time 0 min: 5% solvent B; linear to time 20 min: 0% solvent B, flow rate: 1 mL min^{-1}, and injection volume: 1 μL. MS analysis conditions were: APCI: polarity positive, corona voltage 4000 V, nebulising gas pressure 60 psi, drying gas flow 5 L min^{-1}, vaporizer temperature 400 °C, drying gas temperature 350 °C, capillary voltage 3500 V; ESI: polarity negative, capillary voltage 3500 V, nebulising gas pressure 65 psi, drying gas flow 12 L min^{-1}, drying gas temperature 350 °C; Ion trap: scan 100–3000 m/z; maximum accumulation time, 200 ms, ICC target 10,000. The content of different fractions was quantified as a ratio of the intensity of the areas of the peaks corresponded to m/z in the indicated limits for reacted lignin to the fresh one. Since the conversion of the fractions with m/z higher that 1000 was always smaller than 5%, we will report only the evolution of the fractions with m/z smaller than 1000. Due to some similitude the report was divided in three m/z range categories: 100–500, 500–700 and 700–1000.

3. Results and discussion

3.1. Catalysts characterization

XRD patterns of nickel catalysts indicated that the preparation procedure led to pure 10 nm nanoparticles (Fig. 1b). The characteristic diffraction lines at $2\theta = 44.4°$, 51.7° and 76.5° correspond to

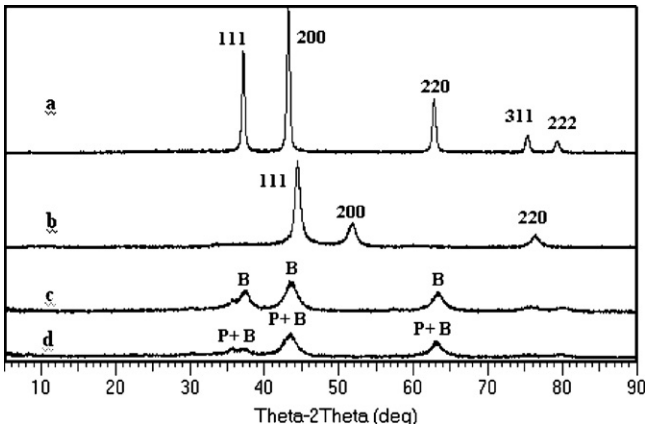

Fig. 1. X-ray powder diffraction patterns of the prepared catalysts: (a) NiO(1 1 1); (b) nano-Ni; (c) Fe_3O_4–$(NiAlO)_x$; (d) Fe_3O_4–$(NiMgAlO)_x$, P–MgO (periclase), B–NiO (bunsenite).

Miller indices (1 1 1), (2 0 0) and (2 2 2) [21] and reveal the existence of a pure face-centered cubic (fcc) phase (JCPDS-004-0850). No lines assigned to oxidized phases or other nickel compounds have been detected. The crystallinity is enough high to eliminate the presence of amorphous phases. Sonochemistry is known to provide a green alternative to the synthesis of nanomaterials with a good control of particle size and morphology [22].

The structure of the NiO nanosheets was also confirmed by the XRD patterns (Fig. 1a). The diffraction lines of (1 1 1), (2 0 0), (2 2 0), (3 1 1), and (2 2 2) faces were identified from the d spacings of 2.4049, 2.0826, 1.4742, 1.2584, and 1.2051 Å, respectively [17] (JCPDS-001-1239). They correspond to a single phase of well-crystallized NiO with the face-centered cubic structure (space group: $Fm3m$) [23]. Coherent scattering regions for nickel oxide were determined by the Scherrer equation [24] based on broadening of diffraction lines (2 0 0), (1 1 1) for NiO. Average size of NiO particles was found as being 19 nm.

The powder XRD patterns of Fe_3O_4–$(NiAlO)_x$ (Fig. 1c) and Fe_3O_4–$(NiMgAlO)_x$ (Fig. 1d) show diffraction lines corresponding to Fe_3O_4 ($2\theta = 30.19$, 35.57, 43.17, 57.12 and 62.79) and NiO ($2\theta = 37.11$, 43.64, 63.09, 75.67 and 79.89). Magnesium and aluminum are silent in these patterns [25].

The reduction of the mixed metal catalysts incorporating Fe_3O_4 with hydrogen does not change the XRD patterns.

However, XPS analysis provided advanced information about the nature of the samples after the reduction in hydrogen. Fig. 2 shows the XPS spectra in the region of the Ni2p binding energy for nano-Ni(0) and NiO(1 1 1). While the energy determined for NiO(1 1 1) corresponds to Ni^{2+} (854 eV) [26] the binding energies determined for the nano-Ni(0) indicated the presence of both Ni^{2+} (854 eV) and Ni(0) (852.5 eV) levels. The reduction of Fe_3O_4–$(NiAlO)_x$ and Fe_3O_4–$(NiMgAlO)_x$ in hydrogen led only to a partial reduction of nickel, and the intensity of the Ni2p3/2 bands assigned to Ni(0)-to-Ni^{2+} had approximately a ratio of 1:3. The deconvoluted XPS spectra for Ni(0) and Ni^{2+} of the two samples are shown in Figs. 1S and 2S (supporting information).

3.2. Lignins extraction and characterization

As its polymeric structure is composed of a variety of monomer units, lignin is considered recalcitrant against most chemical treatment and a major obstacle in processing of plant biomass. Moreover, the isolation method of lignin has an influential role in determining its nature and structure.

Vanderghem et al. [18] have shown that depending on the conditions of the pretreatments, different degrees of delignification were

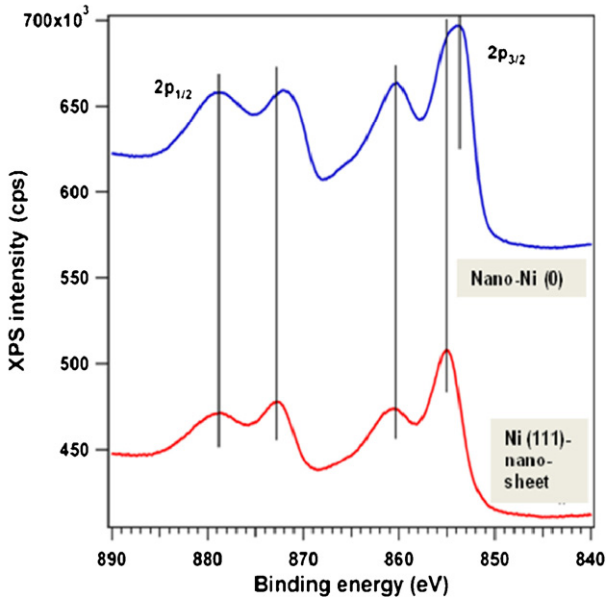

Fig. 2. XPS spectra in the region of the Ni2p binding energy.

obtained from a variety pulps. The acidic pretreatment led to extensive, 86.5%, delignification, while the basic pretreatment led to only 36.3% delignification. The elevated temperatures used in the acidic pretreatment may explain the greater extent of delignification by allowing more lignin to be solvated. Moreover, lignin obtained from acidic pretreatment was more pure, likely due to the dissociation of carbohydrates in the lignin fraction. Therefore, the lignin content, determined by the Klason procedure, was 80% after the acidic pretreatment but only 70% after the ammonia pretreatment [18]. In both FAL and AL samples small amounts of carbohydrates (e.g., pentoses and hexoses) were evidenced and their content depended on the applied pretreatment method. In FAL samples, the level of these compounds was much lower (3.0 wt%) compared to AL samples (13.7 wt%). These differences were explained before [18] by intensive hydrolysis of lignin–carbohydrates bonds resulting in low carbohydrate content for the FAL samples. AL lignin had a noticeable amount of xylan in composition suggesting that xylose may link to lignin by bonds that are resistant to cleavage under basic conditions.

Thermogravimetric analysis indicated the three stages of decomposition reported early by part of the group [18]. First stage, at temperatures below 200 °C, corresponds to evaporation of light compounds (mainly water); the second stage, between 200 °C and 500 °C, corresponds to the liberation of hydrocarbons from the rapid thermal decomposition of hemicelluloses, cellulose and a portion of lignin, and the third stage, above 500 °C, to the steady decomposition of the heavier components of lignin [27]. These results are consistent with the reactivity of the constituent parts [28,29]. Hemicellulose is the most reactive compound while lignin is more thermally stable and starts to decompose at higher temperatures (between 250 and 500 °C).

FTIR spectra were also very similar to the spectra reported by Vanderghem et al. [18]. They contain bands characteristic of carbonyl functional groups, of un-conjugated carbonyl groups and conjugated carbonyl groups (due to both acid hydrolysis and esterification that can take place during the delignification process), of aromatic ring vibrations of the phenylpropene groups, of syringyl units and guaiacyl units. Despite minor deviations, FAL and AL spectra were rather similar, indicating a comparable chemical composition of the extracted lignin samples. The exceptions being the bands located in the carbonyl region at 1760 and 1650 cm^{-1}, where FAL exhibits a higher relative intensity compared to AL. This difference was already assigned to the acid hydrolysis of lignin generating new carbonyl functional groups [30].

Combining these characterizations with HSQC analysis Vanderghem et al. [18] proposed different linkages for AL and FAL. The weight average (M_w) of acetylated lignin samples was reported to be 2760 g mol^{-1} for FAL lignin and 3140 g mol^{-1} for AL lignin. Taking into account that the molecular weight of a phenylpropane unit is 180 g mol^{-1}, the polymerization degree of FAL can be approximated at 15, while the polymerization degree of AL was approximated at a value of 17.

3.3. Analytic measurements

The RPLC mechanism separates compounds in the increasing order of their lipophilic character. The gradient profile starts at 5% acetonitrile in water with 0.1% formic acid and ends at 100% acetonitrile (also containing 0.1% formic acid) over 20 min. Formic acid suppresses ionization of acidic phenolic moieties, avoiding peak broadening and symmetry distortion upon chromatographic elution.

When observing the UV traces at 252 nm, the depolymerised lignin (reaction products) contains a huge number of compounds eluting up to minute 14 (consequently, such compounds are quite polar in nature), while the lignin raw material indicates a less complex pattern, with a group of compounds eluting between minutes 10 and 12. The "hill" profile of the depolymerised lignin (reaction products) between minutes 6 and 14 (similar to GC chromatograms of petroleum fractions) indicates that the 4.75% min^{-1} gradient being applied is still too fast to produce a baseline separation between compounds generated by depolymerisation. It is worthwhile to note that in the conditions of the RPLC separation (even allowing elution with acetonitrile for additional 40 min after the end of the gradient) it is possible that the main congeners from lignin with high molecular masses (>3000) are not eluted from the column at all.

MS detection applied to the lignin raw material and depolymerised lignin (reaction products) revealed that intense responses are obtained under positive (+) APCI and negative (−) ESI conditions. Surprisingly, positive (+) ESI leads to poor responses, disappearing in the baseline noise. APCI mode indicates that the separated compounds have less polar moieties, due to either the loss of phenolic groups or that the ionization is inhibited by the presence of the formic acid. The (−) ESI probably detects compounds having phenolic groups with a low pK_a. Note that the mass scan was limited to 3000 amu. The averaged mass spectra obtained over the whole chromatogram (monitored either in (+) APCI or (−) ESI conditions) indicates that compounds eluting near 20 min (almost the end of the gradient profile) have masses in the 50–350 amu range, while compounds eluting during the isocratic, 100% acetonitrile, step exhibited masses greater than 350 amu. These affirmations are based on the assumption that little molecular fragmentation arises in the APCI sources due to milder the ionization conditions. The groups of peaks eluting after 20 min have similar MS patterns that have characteristic signals separated by fixed distances (44 corresponding to a CO_2 loss, 28 for CO, or 18 for water could be observed). This indicates that compounds within a group belong to homologous series differing by a carboxyl or a carbonyl group. Compounds detected under (−) ESI conditions were lighter ones, as their chromatographic retention time is less than 20 min. For exemplification, illustrative figures showing APCI and ESI mass spectra were included in the supplementary material (Figs. 3S and 4S).

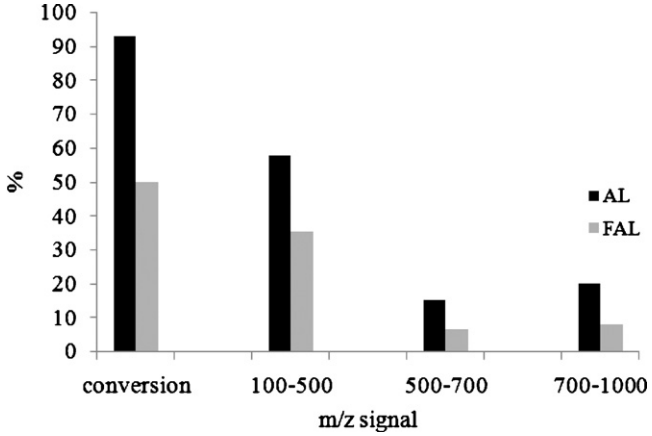

Fig. 3. Depolymerization of lignin under autoclave conditions (catalyst: 0.02 g nano Ni, 0.16 g lignin, IL: 2 g [BMIM]OAc, 10 atm H_2, 180 °C, 24 h).

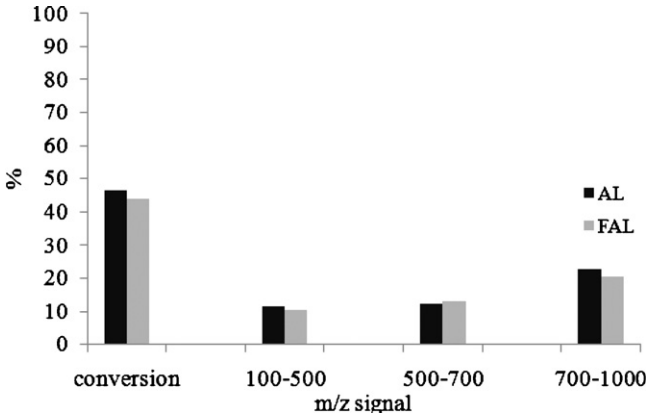

Fig. 5. Depolymerization of lignin samples under ultrasound conditions (catalyst: 0.27 g nano-Ni, 0.25 g lignin, 30 mL water, 6 h).

3.4. Catalytic behavior

3.4.1. Depolymerization on Ni(0)

Blank experiments in the absence of the catalysts showed that the lignin was fragmented neither under autoclave nor under the ultrasound activation.

Fig. 3 shows the conversion of AL and FAL, and distribution of products with masses below 1000 amu on the nano-Ni(0) catalyst. Under the indicated conditions, the conversion of AL reached a higher value (around 90% of the initial amount of lignin was depolymerized) compared to FAL. 60% of the products shown are between 100 and 500 *m*/*z*. This behavior is supported by the structures proposed by Vanderghem et al. [18] for AL and FAL samples. Nickel may more easily catalyze the hydrogenolysis of ethers in AL, than the α,β-unsaturated esters in FAL. The high conversion rate could also be a function of particle size, the nanoparticles may be able to penetrate deeper into the polymeric network of lignin and, consequently, could more efficiently disrupt the linkages between the lignin monomers.

Figs. 4–6 present the catalytic behavior of the same catalyst under ultrasonic activation in different solvents. Like in the autoclave experiments, in all the cases the conversion of AL was superior to the conversion of FAL, supporting the hypothesis the reaction mechanism does not depend on the way the reaction has been activated. However, irrespective of the nature of the solvent that has been employed, all the experiments show the extent of depolymerization was greatest under autoclave conditions. The advanced solubilization of lignin and the hydrogen pressure may be responsible for this behavior. It is worth mentioning that the amount of the catalyst used under ultrasonic conditions was almost 10 times greater than that used in an autoclave.

However, it is difficult to compare the two reaction methodologies. Under autoclave conditions no or very poor results were obtained by using an organic solvent in which lignin is not soluble or only partly soluble. In both cases, in the reaction medium, only a dispersion of two solids (lignin and catalyst) has been observed. Therefore, almost no interactions between lignin and catalyst will be possible, because the solid particles of the lignin, consisting of polymeric chains, are not able to enter the pore system. Under autoclave conditions the interaction of lignin with the catalyst become possible since the lignin is soluble in IL. Contrarily, under ultrasounds conditions, solvents in which lignin is only partly soluble or totally insoluble can be used as long as the lignin particles are fragmented under the ultrasounds effects.

On the other side, it is well known that in sonochemistry, in most of the cases, high temperatures are not necessary to accelerate a chemical process. Under autoclave conditions the activation is different, and therefore, because of the high cross-linked polymer form, the lignin breakdown requires elevated temperatures. Working under ultrasounds conditions, our experimental set-up does not support a high pressure as it is the case of autoclave.

Generally, sonochemistry in heterogeneous systems is the result of a combination of chemical and mechanical effects of cavitation, and it is very difficult to ascribe sonochemistry to any single global origin, other than the overriding source of activity, namely, cavitation [31]. Whatever the mechanism is (i.e. chemical and mechanical

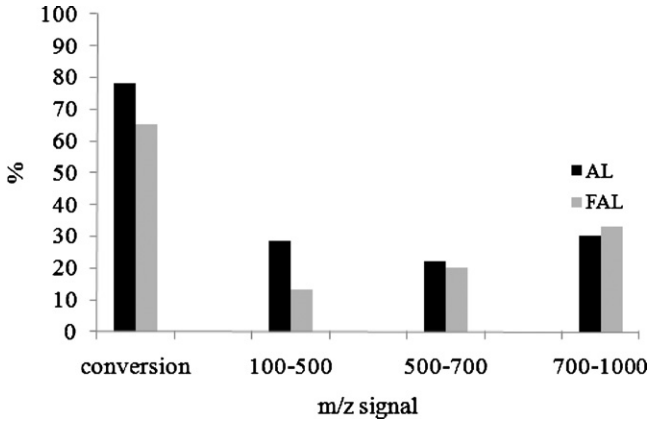

Fig. 4. Depolymerization of lignin samples under ultrasound conditions (catalyst: 0.27 g nano-Ni, 0.25 g lignin, 30 mL methanol, 6 h).

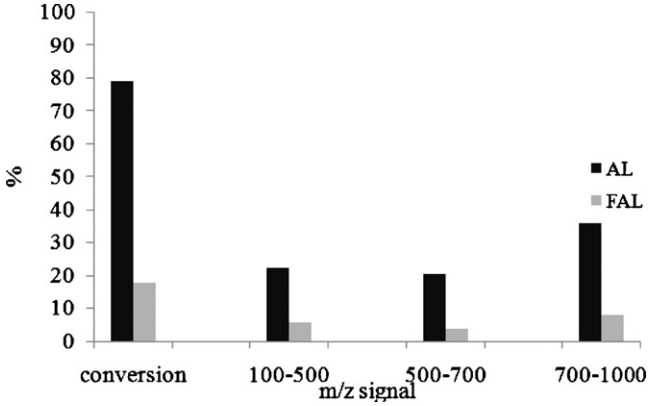

Fig. 6. Depolymerization of lignin samples under ultrasound conditions (catalyst: 0.27 g nano-Ni, 0.25 g lignin, 30 mL ethyl acetate, 6 h).

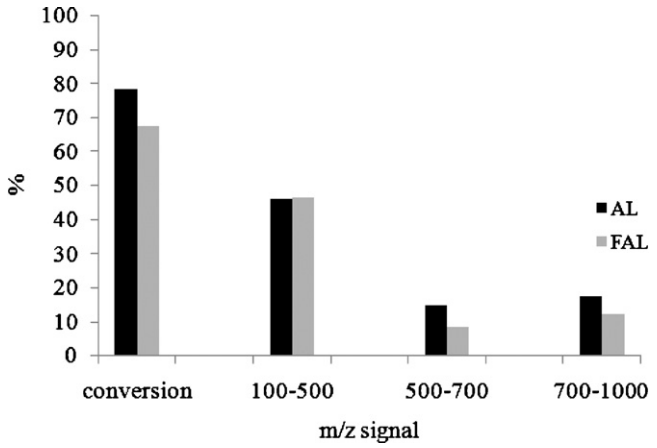

Fig. 7. Depolymerization of FAL and AL samples under autoclave conditions (catalyst: 0.02 g $(NiAlMgO)_x$, 0.16 g lignin, IL: 2 g [BMIM]OAc, 10 atm H_2, 180 °C, 24 h).

effects of cavitation) the real benefit of using ultrasound lies in its unique selectivity and reactivity enhancement.

Data presented in Figs. 4–6 shows changes in selectivity compared to the experiments carried out in autoclave conditions. Under ultrasonic activation the distribution of the products between 100 and 1000 *m*/*z* is not influenced by any of the solvents used.

The nature of the solvent was also found to exhibit a small effect on these reactions, except for ethyl acetate, the conversion of AL samples was greater. The extent of lignin depolymerization varied in the order methanol > ethyl acetate > water. This could imply that methanol interacts with the disrupted fragments and favors a more advanced depolymerization. Transesterification of ethyl acetate is also plausible.

3.5. Depolymerization on Ni oxide catalysts

Figs. 7 and 8 show catalytic results of Fe_3O_4–$(NiAlO)_x$ and Fe_3O_4–$(NiMgAlO)_x$ catalysts under autoclave conditions. Although AL still shows higher conversions than FAL, the difference between the conversion of AL and FAL is less than the difference measured using nano-Ni(0) catalysts. This is also apparent in the distribution of the products between 100 and 1000 *m*/*z*. The presence of magnesium (Fig. 7) led to an increase in the conversion but with this catalyst the products between 100 and 500 *m*/*z* was decreased.

Figs. 9 and 10 show comparative results in depolymerization of FAL and AL using nano-Ni(0) and NiO(1 1 1) under ultrasound activation in methanol. These data show rather small differences

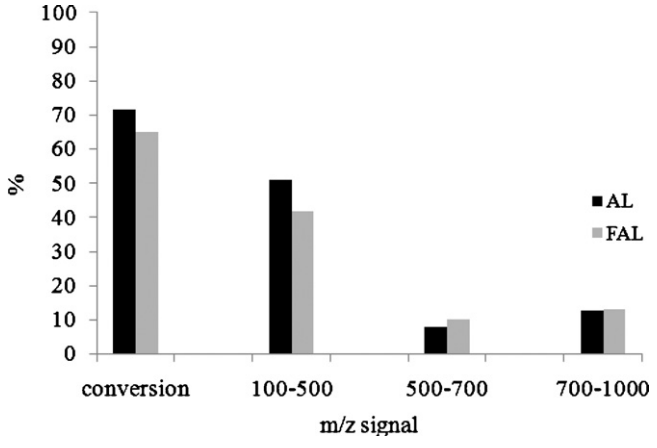

Fig. 8. Depolymerization of FAL and AL samples under autoclave conditions (catalyst: 0.02 g $(NiAlO)_x$, 0.16 g lignin, IL: 2 g [BMIM]OAc, 10 atm H_2, 180 °C, 24 h).

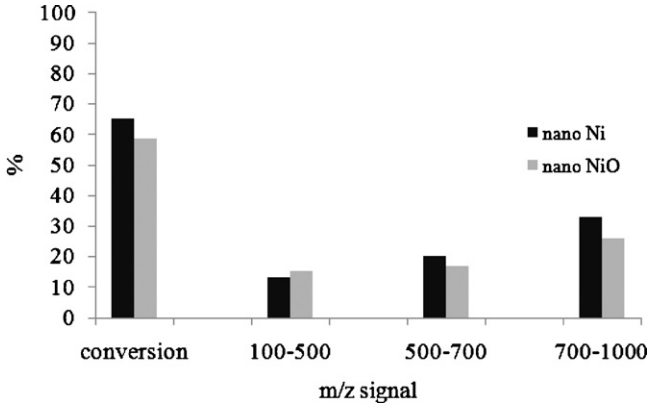

Fig. 9. Depolymerization of FAL under ultrasound conditions (catalyst: 0.27 g nano-Ni or 0.27 g NiO, 0.25 g FAL lignin, 30 mL methanol, 6 h).

between the two catalysts. Such a behavior may account for at least a partial reduction of NiO(1 1 1) under hydrogen bubbled atmosphere and ultrasound activation.

3.6. General assessments

Reaction of lignin under pressurized hydrogen at elevated temperatures and in the presence of a suitable catalyst is one of the most intriguing approaches for lignin depolymerization and hydrodeoxygenation [1]. Shabtai et al. [32] proposed a three-step process for converting lignin into reformulated gasoline. Including base-catalyzed depolymerization (BCD) followed then by hydrodeoxygenation and hydrocracking. When chemicals are the target products, the process may be ended before the final step and the phenolics can be extracted from the product after hydrodeoxygenation [32].

The proposed BCD process has two distinct disadvantages: the use of strong homogeneous base catalysts and the energy input required. Replacing the homogeneous catalyst with a heterogeneous solid base catalyst, such as those used in this work (i.e. $(NiAlMgO)_x$, $(NiAlO)_x$, NiO(111), nano-Ni(0)) could have the advantage of avoiding waste productions and the separation of the homogeneous catalyst. Moreover, the magnetic properties of materials incorporating Fe_3O_4 provide an easier separation method and allow for recycling of the catalyst. The use of nanostructured catalysts may also have other advantages such as higher reactivity or better dispersion into the reaction mixture.

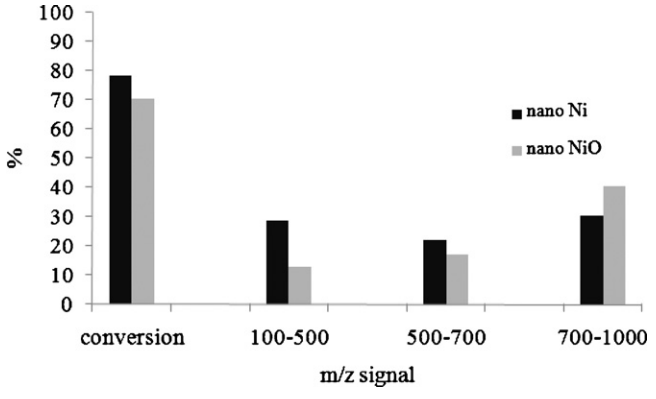

Fig. 10. Depolymerization of AL under ultrasound conditions (catalyst: 0.27 g nano-Ni or NiO, 0.25 g AL lignin, 30 mL methanol, 6 h).

The characterization of the catalysts indicated that nickel can exist in nanoparticles in a zero-valent oxidation state (nano-Ni(0)), oxidized state (NiO(1 1 1)), or a mixture of reduced and oxidized states ($(NiAlMgO)_x$ and $(NiAlO)_x$).

The currently accepted structure of lignin consists of three basic monomers (coniferyl, sinapyl and *p*-coumaryl alcohols) connected by β-*O*-4, α-*O*-4, β-5, 5-5, 4-*O*-5, β-1 and β-β linkages [33]. However, as the characterization of the lignin samples has shown, the proportion of these monomers is different as a function of the applied procedure (FAL or AL). Previous studies have shown that β-*O*-4 and α-*O*-4 linkages in lignin are easily cleaved, while the 5,5-(biphenyl)-type and aromatic ring structures are more stable [34]. This data agrees with the results presented here. Showing that irrespective of the catalyst, the extent of depolymerization in AL was higher than the extent of depolymerization in FAL. These results are more interesting from a practical point of view taking into consideration the molecular weight of AL is higher than that of FAL, the low-molecular weight fraction (m/z = 100–500) preponderated, and it was followed by the fraction with m/z of 700–1000.

The activation of the catalysts is also very important. The chemical effects of a sonochemical reaction result from acoustic cavitation, defined as the formation, expansion, and rapid implosion of bubbles. The bubbles create transient localized hot spots upon implosion with extremely high temperature and pressure [35]. The experiments carried out in an autoclave led to better results compared to ultrasonic activation. Under ultrasonic activation the solid surfaces (especially powders) collapse because enough energy is produced to cause fragmentation, even for nanostructured materials. Such an effect takes place in these reactions for both the lignin and the catalyst. In the case of the catalyst this effect may lead to an increased active surface area and may favor efficient mixing and enhanced mass transport. For very fine powders, as in the case of nano-Ni catalyst, the particles are accelerated to high velocity by cavitational collapse and may collide to cause surface abrasion. These phenomena may generate particles with different sizes, as well as the agglomeration of small particles. The rearrangement of solid particles (i.e. fragmentations, agglomeration) may affect the catalytic performance leading, in many cases, to a decrease in the catalytic activity. In the case of lignin, irrespective of the preparation procedure that has been employed, the low molecular weight monomers (m/z = 100–500) may suffer a polymerization to higher molecular weight monomers (m/z = 700–1000) (see Figs. 4–6).

4. Conclusions

Lignin isolated from *Miscanthus* × *giganteus* using acidic (FAL) and alkali (AL) conditions was thereafter subjected to catalytic depolymerization under thermal or ultrasonic activation. The characterization of lignins was achieved by thermogravimetric analysis and FTIR. Three different classes of catalysts, containing nickel as active species, have been prepared in this scope: (i) nano-Ni by reduction of $NiCl_2$ with $NaBH_4$ under ultrasonication, (ii) Fe_3O_4–$(NiMgAlO)_x$ and $(NiAlO)_x$ by calcination of Mg(Ni)–Al hydrotalcite incorporating Fe_3O_4 followed by reduction with hydrogen, and (iii) NiO(1 1 1) nanosheets by reduction of $Ni(NO_3)_2$ with urea using benzyl alcohol as a structure directing agent. The catalysts were characterized by XRD and XPS techniques. Reduced mixed oxides displayed a moderate activity while a significant increase in conversion (up to 90%) was observed in the presence of nano-Ni(0). NiO(1 1 1) nanosheet catalysts performed very close to nano-Ni(0). The conversion and the mass distribution of the reaction products were strongly related to the procedure used for the extraction of lignin samples. In all the cases AL led to a greater extent of depolymerization. The performances of the tested catalysts under ultrasound conditions were inferior to those tested under conventional heating conditions. The nature of the solvent was also found to be very important in this process, with the ionic liquid [BMIM]OAc leading to the best results under autoclave conditions, and methanol under ultrasonic conditions. In all the cases the conversion of the fractions with m/z higher than 1000 was smaller than 5%.

Acknowledgements

The authors kindly acknowledge the American Chemical Society (ACS) for the ACS GREET pilot program grant in 2011 awarded to Kenneth Finch to study at the Department of Organic Chemistry, Biochemistry and Catalysis of University of Bucharest, under host Professor Dr. Simona Coman. Part of the work was supported by the strategic grant POSDRU/89/1.5/S/58852, Project "Postdoctoral programme for training scientific researchers" co-financed by the European Social Foundation within the Sectorial Operational Program Human Resources Development 2007–2013. Aurore Richel is grateful to the "Région Wallonne" (Belgium) for its financial support ("Technose" Excellence Programme). The authors are also grateful for the support of COST (UBIOCHEM action) and the STSM of Dr. Marian Verziu.

Appendix A. Supplementary data

Supplementary data associated with this article can be found, in the online version, at doi:10.1016/j.cattod.2012.02.051.

References

[1] M.P. Pandey, C.S. Kim, Chem. Eng. Technol. 34 (2011) 29–41.
[2] S. Baumlin, F. Broust, F. Bazer-Bachi, T. Bourdeaux, O. Herbinet, F. Toutie Ndiaye, M. Ferrer, J. Lédé, Int. J. Hydrogen Energy 31 (2006) 2179–2192.
[3] B.N. Kuznetsov, M.L. Shchipko, Bioresour. Technol. 52 (1995) 13–19.
[4] H. Yang, R. Yan, H. Chen, D. Ho Lee, C. Zheng, Fuel 86 (2007) 1781–1788.
[5] S. Nenkova, T. Vasileva, K. Stanulov, Chem. Nat. Compd. 44 (2008) 182–185.
[6] H. Deng, L. Lin, Y. Sun, C. Pang, J. Zhuang, P. Ouyang, Z. Li, S. Liu, Catal. Lett. 126 (2008) 106–111.
[7] C. Crestini, M.C. Caponi, D.S. Argyropoulosc, R. Saladino, Bioorg. Med. Chem. 14 (2006) 5292–5302.
[8] S. Wang, K. Wang, Q. Liu, Y. Gu, Z. Luo, K. Cen, T. Fransson, Biotechnol. Adv. 27 (2009) 562–567.
[9] C.A. Mullen, A.A. Boateng, Fuel Process. Technol. 91 (2010) 1446–1458.
[10] T. Furusawa, T. Sato, H. Sugito, Y. Miura, Y. Ishiyama, M. Sato, N. Itoh, N. Suzuki, Int. J. Hydrogen Energy 32 (2007) 699–704.
[11] W.-J. Xu, W. Zhao, C. Sheng, S.-T. Zhong, X.-N. Wu, C.-H. Yan, S. Bai, Z.-M. Zong, X.-Y. Wei, Energy Fuels 24 (2010) 250–252.
[12] J. Zhang, H. Deng, L. Lin, Molecules 14 (2009) 2747–2757.
[13] J.D.P. Araújo, C.A. Grande, A.E. Rodrigues, Chem. Eng. Res. Des. 88 (2010) 1024–1032.
[14] Y. Pu, N. Jiang, A.J. Ragauskas, J. Wood Chem. Technol. 27 (2007) 23–33.
[15] J. Zakzeski, A.L. Jongerius, B.M. Weckhuysen, Green Chem. 12 (2010) 1225–1236.
[16] N. Yan, C. Zhao, P.J. Dyson, C. Wang, L.-tao Liu, Y. Kou, ChemSusChem 1 (2008) 626–629.
[17] J. Hu, K. Zhu, L. Chen, H. Yang, Z. Li, A. Suchopar, R. Richards, Adv. Mater. 20 (2008) 267–271.
[18] C. Vanderghem, A., Richel, N., Jacquet, Ch. Blecker, M. Paquot, Polym. Degrad. Stab. doi:10.1016/j.polymdegradstab.2011.07.022.
[19] H.Q. Lam, Y. Le Bigot, M. Delmas, G. Avignon, Ind. Crop. Prod. 4 (2001) 139–144.
[20] J. Wang, J. You, P. Yang, C. Zhong, Z. Li, M. Zhang, X. Jing, Mater. Sci.: Poland 26 (2008) 591–599.
[21] Z.-F. Zhao, Z.-J. Wu, L.-X. Zhou, M.-H. Zhang, W. Li, K.-Y. Tao, Catal. Commun. 9 (2008) 2191–2194.
[22] J.A. Dahl, B.L.S. Maddux, J.E. Hutchison, Chem. Rev. 107 (2007) 2228–2269.
[23] Y. Diao, W.P. Walawender, C.M. Sorensen, K.J. Klabunde, T. Ricker, Chem. Mater. 14 (2002) 362–368.
[24] R.T.K. Baker, Carbon 27 (1989) 315–323.
[25] L. Obalova, K. Jiratova, F. Kovanda, M. Valaskova, J. Balabanova, K. Pacultova, J. Mol. Catal. A: Chem. 248 (2006) 210–219.
[26] M.G. Cook, N.S. McIntyre, Anal. Chem. 47 (1975) 2208–2213.
[27] S.S. Abdullah, S. Yusup, M.M. Ahmad, A. Ramli, L. Ismal, Int. J. Chem. Biol. Eng. 3 (2010) 137–141.
[28] Y. Wu, Z.L.H. Zhao, F. He, J. Fuel. Chem. Technol. 37 (2009) 427–432.
[29] A. Uslu, A.P.C. Faaij, P.C.A. Bergman, Energy 33 (2008) 1206–1223.

[30] L. Serrano, I. Egües, M. González Alriols, R. Llano-Ponte, J. Labidi, Chem. Eng. J. 156 (2010) 49–55.
[31] M. Doble, A.K. Kruthiventi, Green Chemistry & Engineering, Elsevier Science & Technology Books, 2007.
[32] J.S. Shabtai, W.W. Zmierczak, E. Chornet, US Patent 5959167 (1999).
[33] J. Zakzeski, P.C.A. Bruijnincx, A.L. Jongerius, B.M. Weckhuysen, Chem. Rev. 110 (2010) 3552–3599.
[34] A. Tejado, C. Pena, J. Labidi, J.M. Echeverria, I. Mondragon, Bioresour. Technol. 98 (2007) 1655–1663.
[35] K.S. Suslick, T. Hyeon, M. Fang, Chem. Mater. 8 (1996) 2172–2179.